Biomass Conversion and Biorefinery (2024) 14:21273–21282
https://doi.org/10.1007/s13399-023-04137-5

ORIGINAL ARTICLE

# A non-woven waste cellulosic fibers–iron shavings abrasive composite: synthesis, characterization, and evaluation of its wear mechanism

**Arwa Elaissi[1] · Mahjoub Jabli[1,2] · Adel Ghith[1]**

Received: 7 February 2023 / Revised: 17 March 2023 / Accepted: 24 March 2023 / Published online: 5 April 2023


## Abstract

Iron scrap is one of the substances rejected in large quantities of by-products from the steel industrial sector. In this work, waste cellulosic fibers and iron shavings were used as reinforcement and abrasive particles, respectively. Two methods of the synthesis of the hybrid composites were applied namely spraying and coating. Different analytical techniques of characterization, i.e., Fourier-transform infrared (FT-IR) spectroscopy, scanning electron microscopy (SEM), thermogravimetric analysis (TGA/DTG), and energy-dispersive X-ray (EDX), were used to analyze the studied samples. The morphology of the abrasives displayed the presence of spherical grains on the surface with a diameter ranging from 100 to 200 µm. In the spraying process, the surface was characterized by the presence of hollows, bumps, and small empty areas. For the coating process, the fibers of the reinforcement and some drops of resins were visible on the surface of the abrasives. The EDX analysis suggested that the abrading action of the composite surface might be done by tearing off the iron grains. The properties of the matrices, process considered, size of the grains, and their distribution were found to be the principal parameters governing the abrasive process. As the particle size increases, the surface becomes rougher, allowing for more scraping of the materials surfaces.

**Keywords** Waste cellulosic fibers · Iron shavings · Reinforcement · Spraying · Coating · Surface roughness

## 1 Introduction

Surface defects and surface roughness are present in any manufactured material. This unevenness needs to be removed from the surface in attempts to obtain acceptable surface requirements. The combination of particle size, surface roughness, and adhesion between phases are some factors of abrasive performances under numerous tribological situations [1, 2]. In addition, the quality of the prepared abrasives is mainly affected by chemical composition, and abrasive microstructure, as well as the manufacturing process, and production conditions [3]. Hard protuberances or implanted stiff particles cause two-body abrasion. Whereas, in three-body abrasion, the hard particles can move freely (roll or slide) across the contacting surfaces. The rate of material removal in three-body abrasion can be an order of magnitude lower than in two-body abrasion. This is because the loose abrasive particles only wear down the solid surfaces between which they happen only about 10% of the time, compared to 90% in bi-body abrasion [4].

Waste dumped in large quantities by industries creates serious environmental problems. At the lowest possible environmental impact, the reuse of this waste will become an essential standard for protecting the environment [5]. Iron scrap is one of the substances rejected in large quantities of by-products from the steel industrial sector. It is the most common metal used in everyday life, usually in the form of various alloys. It is characterized by its solidity which gives

**Highlights**
- Waste fibers and iron shavings were used as reinforcement and abrasive particles.
- Two methods of the synthesis were applied: spraying and coating.
- FT-IR, SEM, TGA/DTG, and EDX were used to analyze the studied samples.
- EDX exhibited that spray method produced a higher rate of iron compared to coating method.

✉ Mahjoub Jabli
m.jabli@mu.edu.sa

[1] Textile Materials and Processes Research Unit (MPTEX), National Engineering School of Monastir, University of Monastir, Monastir, Tunisia

[2] Department of Chemistry, College of Science Al-Zulfi, Majmaah University, 11952, Al-Majmaah, Saudi Arabia

it an abrasive character. Various techniques have reportedly been tried to make operational use of scrap iron and steel throughout the history of the iron and steel industries. Numerous studies have been done on using garbage in the concrete mix to enhance the qualities of the concrete and keep these unwanted components out of the environment. Iron ore tailings could replace some of the concrete aggregate used in stiff pavements [6]. In an experimental study, Ghannam et al. had reported the viability of replacing some of the fine aggregates in the concrete mix with iron and granite powder [7]. To improve the strength of concrete, scrap metal was used in the research of Krirak et al., as a partial replacement for sand in concrete [5].

Recently, the micromachining technique known as magnetic field-assisted manufacturing was developed for engineering materials appropriate for industrial functions [8, 9]. Ahmad et al. used these findings to a magnetic abrasive made of iron and alumina particles designed for fluid machining. Results indicated that combining big iron particles in a given quantity could reduce surface roughness [10]. Polishing performance is influenced by the abrasive type, morphology, roughness, size distribution, and mechanical characteristics, among other factors [11]. A theoretical study on modeling and simulation of the magnetic abrasion finishing process is conducted by Jayswal et al. [12]. A magnetic fluid was used to clean a curved surface by Suzuki et al. [13, 14].

As a new contribution to the current context, we prepare herein a new high-performance abrasive, non-woven waste cellulosic fibers–iron shavings abrasive composite, at a lower cost from industrial waste. Indeed, the scrap metal, due to its high strength, roughness, and durability, is reused as abrasive grains. A non-woven made from natural fiber waste is employed as reinforcement. The low cost and density, relatively high stiffness, and reusability constitute the principal criteria influencing the widespread use of these materials in composites application. The effect of the choice of used materials, choice of the abrasive manufacturing process on polishing force and MRR, and the abrasives abrasion were explored in this study to obtain the optimum surface conditions in a high yield. SEM, EDX, TGA/DTG, and roughness measurements were used to perform a thorough analysis of the microstructure and abrasion mechanism.

## 2 Experimental

### 2.1 Materials

Grains of iron scrap were collected from a local market (Industrial zone, Monastir-Tunisia), washed, dried, and examined to determine the desired grain size. The powdered grains are less than 0.2 mm in size. Grains with a size between 0.2 and 0.4 mm are selected as medium sizes and big grains are considered as greater than 0.4 mm. The non-woven used as support is composed of cotton and tow (50/50). Three commercial resins are studied as binders namely Recacryl M resin with PAZ catalyst (acrylic resin), Politex resin (polyurethane resin), and R-245 (polyester resin). Their properties were described in previous works [15, 16].

### 2.2 Abrasives manufacturing

In this study, two methods are employed to manufacture abrasives namely spraying and enduction. For the spray process, the resin and the catalyst mixture are dosed and injected using an air pressure spray cannon. Following that, the grains are injected using the same procedure [17]. This open mold process is used for making boats, tanks, transportation components, and ship pieces in a variety of structures [18]. Concerning the enduction process, the solution is poured progressively over the textile material once the reinforcement is secured on the coating table. The second coat of resin is then fully mixed with the abrasive grains. The third layer of grains is spread all along the surface. The film thickness is determined by the coating application technique. After that, each sample was dried at the polymerization temperature for just an appropriate period. Eighteen samples were manufactured according to the characteristics indicated in Table 1.

Figure 1 gives some photographs of the virgin products and produced non-woven materials.

**Table 1** A summary of the used resins, grains size, processes, and the characteristics of the prepared non-woven materials

| Samples | Resin | Grains | Process |
|---|---|---|---|
| 1 | Politex | Small size | Spraying |
| 2 | Resacryl M | Small size | Spraying |
| 3 | Polyester | Small size | Spraying |
| 4 | Politex | Medium size | Spraying |
| 5 | Resacryl M | Medium size | Spraying |
| 6 | Polyester | Medium size | Spraying |
| 7 | Politex | Large size | Spraying |
| 8 | Resacryl M | Large size | Spraying |
| 9 | Polyester | Large size | Spraying |
| 10 | Politex | Small size | Enduction |
| 11 | Resacryl M | Small size | Enduction |
| 12 | Polyester | Small size | Enduction |
| 13 | Politex | Medium size | Enduction |
| 14 | Resacryl M | Medium size | Enduction |
| 15 | Polyester | Medium size | Enduction |
| 16 | Politex | Large size | Enduction |
| 17 | Resacryl M | Large size | Enduction |
| 18 | Polyester | Large size | Enduction |


**Fig. 1** Photographs showing virgin products and produced non-woven materials

## 2.3 Characterization instruments

FT-IR spectra were used to analyze the chemical compositions of the studied materials and identify the various functional groups present in various abrasives using a Perkin Elmer spectrometer. Spectra have been recorded between 4000 and 400 $cm^{-1}$ to have a decent resolution of the spectrum.

The specimens were scanned using an FEI Q250 Thermofisher instrument operating at 25 kV with various magnifications to compare the various characteristics of composites and analyze the interplay between the matrix and reinforcement between polishing. To perform this research, the sample must be metalized, which involves covering it with a layer of gold to make it conductive. As a result, the sample is emptied and subjected to an electric current generated by a cathode. Signals are produced when the sample and beam interact, and these signals are then captured and amplified to produce the image.

The elemental composition of the studied materials was determined using energy-dispersive X-ray analysis. The EDX testing was coupled with SEM.

The thermal decomposition of composite materials was examined in a nitrogen environment at a rate of 10 °C/min from 25 to 700 °C. The curves were recorded on a Perkin Elmer device instrument.

Roughness is the parameter quantifying the 3D geometry of the surface of the systems. In this investigation, a Universal Surface Tester (UST, Innowep®) was used to measure the surface roughness parameter $R_a$ of the studied composites. The UST characterization of samples ($1 \times 1$ $cm^2$ zone) is analyzed using a steel ball 20 mm in diameter. The 0.1 mm/s speed machine results in a point being captured every 0.5 mm.

The abrasive wear tests (ISO 12947) were performed in a dry state with a load of 9 N at a constant speed of 200 mm/s [19]. All produced composites were subjected to a 5000

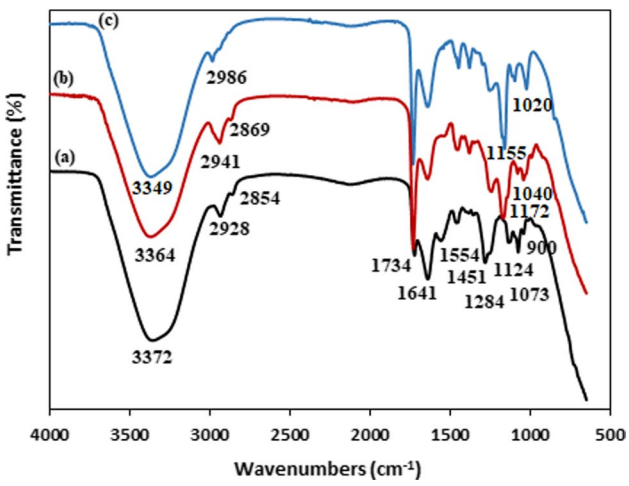


**Fig. 2** FT-IR spectra of abrasives: (**a**) non-woven Politex and iron medium grains, (**b**) non-woven Polyester and iron medium grains, and (**c**) non-woven Resacryl M and iron medium grains

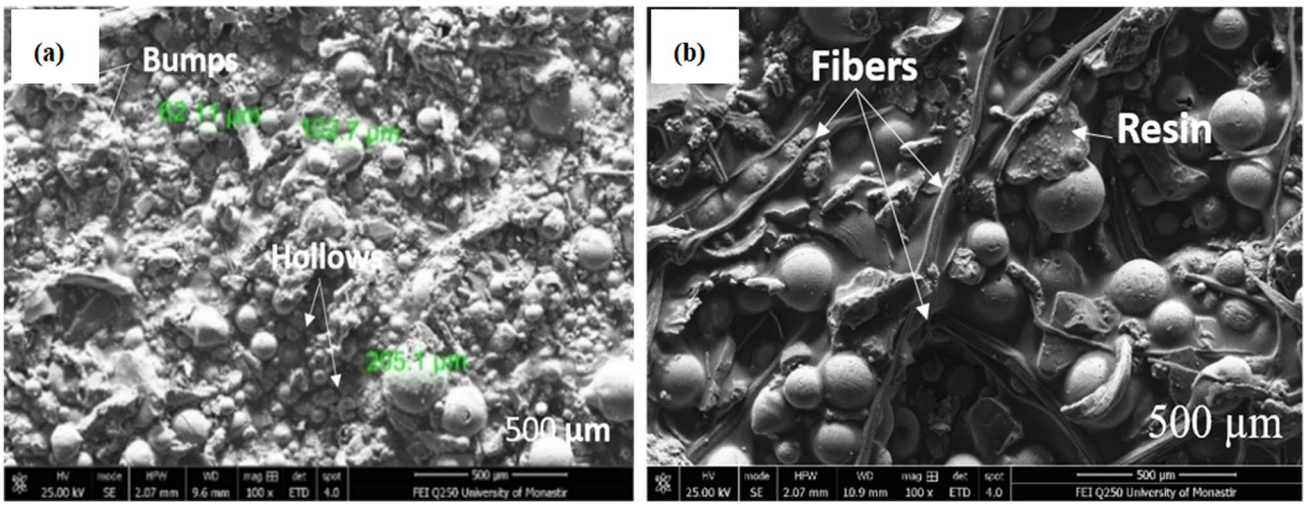


**Fig. 3** SEM images of the abrasive manufactured by medium grains and politex resin using (**a**) spraying and (**b**) enduction processes

cycle abrasion test to degrade the denim fabric. The particular wear rate can be determined using weight loss and thickness data before and after polishing [20]. An average value was calculated after five measurements for each condition.

## 3 Results and discussion

### 3.1 FT-IR characterization

The spectra of the samples prepared using medium iron grains and the three studied resins are given in Fig. 2. According to the spectrum of abrasives made by Politex resin, Fe–O stretching is shown in the range of 900–300 $cm^{-1}$ [21]. Namdouri et al. [22] demonstrated that Goethite (α- FeOOH) can be taken into account at the pic of 1124 $cm^{-1}$ [23]. Band characteristic of hydroxyl groups was observed in the region of 3372 $cm^{-1}$. Trovati et al. [24] attributed the two bands around 2938 and 2854 $cm^{-1}$ to symmetric and non-symmetric stretching of the methyl and methylene groups. According to Pathania et al. [25], C-H bending is shown at 1155 $cm^{-1}$. In the research of Misawa et al. [26], the first oxides to develop when the iron is exposed to the atmosphere are Fe oxyhydroxides, which are oxidized from Fe(II) complexes. In the case of acrylic resin, we denote the presence of vinyl patterns. Indeed, the peak observed at 1697 $cm^{-1}$ could be assigned the C = C group. Qinhuo [27] specified that

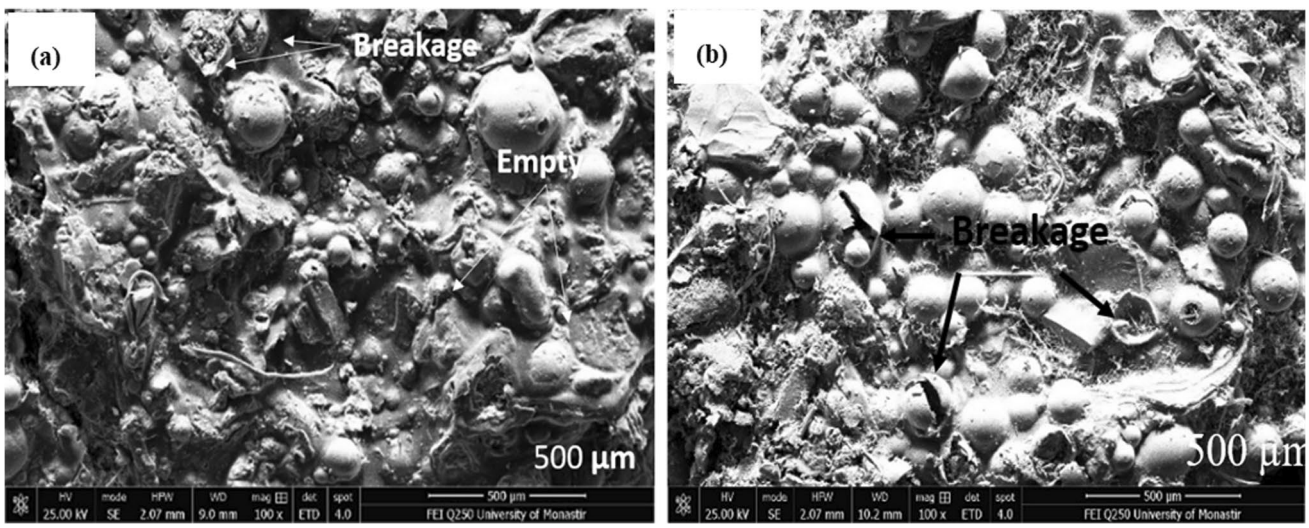


**Fig. 4** SEM images of abrasive manufactured after polishing made by medium grains, and Politex resin using:(**a**) spraying and (**b**) enduction processes

the acrylic agent has a peak characteristic at 1100 $cm^{-1}$ -1150 $cm^{-1}$ which is attributed to the alkyl stretch band group (C–O–C). The band at 1750 $cm^{-1}$ corresponds to the C = O group.

### 3.2 Morphology analysis

Figure 3 shows the abrasive surface made by medium grains, politex resin, and prepared by pulverization and enduction methods, respectively. The morphology of the surfaces shows that the grains are spherical. Using the spraying process, the appearance of hollows and bumps is due to the maldistribution of grains. There is some grain buildup in areas and small empty areas [28]. This result was predictable since the grains are produced by a spray gun. Regarding the coating process, the fibers of the reinforcement are visible on the surface of the abrasives. Also, drops of resins can be observed on the surface of the abrasives. This result is due to the application of a mixed layer of resin and grains.

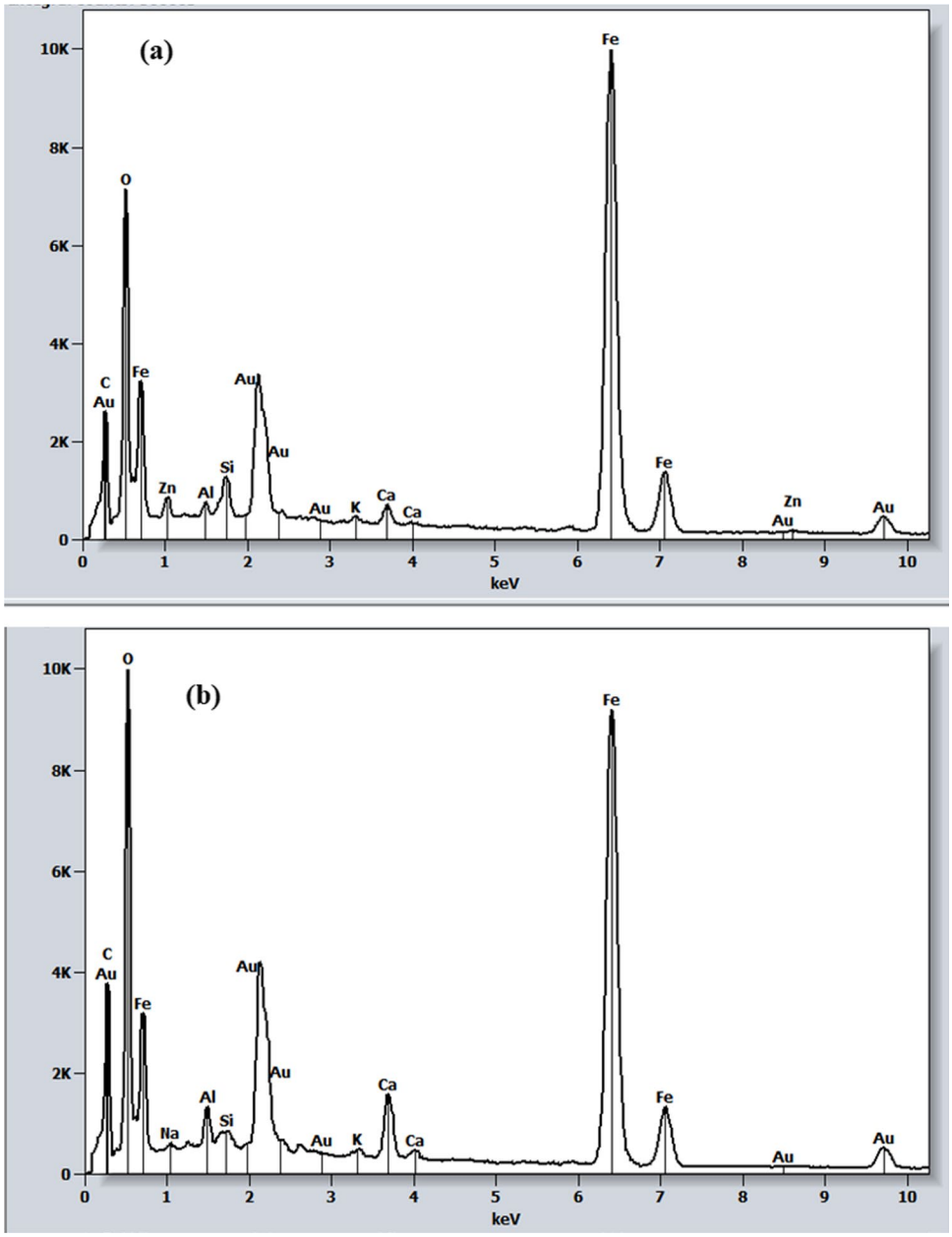


**Fig. 5** EDX analysis of manufactured abrasive before abrasion made by medium grains, and Politex resin using (**a**) spraying and (**b**) enduction processes

Figure 4 shows the surfaces of abrasives used after the abrasion test. In fact, SEM images display the disappearance or breakage of a few grains. The manufacture of abrasives by the coating process generates an improved surface compared to those obtained by the spraying process. This is because the spray gun makes it possible to arbitrarily inject the grains onto the surface. On the contrary, the coating table makes it possible to spread the grains in a homogeneous way all along the surface.

### 3.3 EDX analysis

Figure 5 shows the EDX images taken at the initial state of the abrasives made by medium grains and politex resin using spraying and enduction processes. As it is observed, the intensity of the peak related to the presence of iron is more important for the spray method as compared to the enduction method. This trend could be explained by the fact that the compaction nature of the grains by spray gun results in the accumulation of metallic grains in the same area. On the contrary, the coating process allows, on the surface, a layer mixed with resin and grains [29]. The spectra displayed also the presence of other elements including aluminum. The elemental analysis of this specimen revealed particles containing mainly carbon, oxygen, and iron. The element Au observed in the spectrum is intended for the metallization of samples by gold. Also, aluminum, silicon, potassium, and

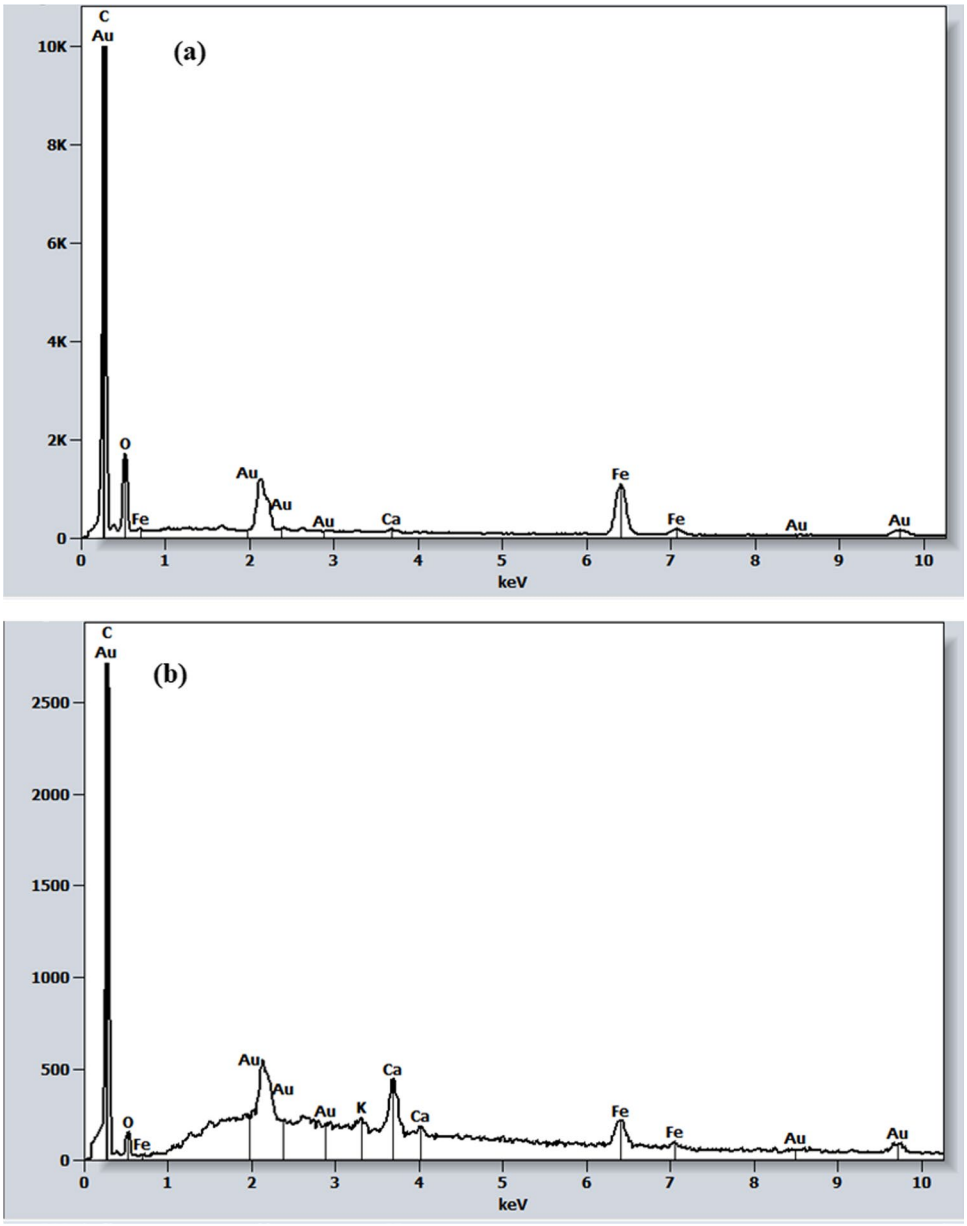


**Fig. 6** EDX analysis of manufactured abrasive after abrasion by medium grains and Politex resin using (**a**) spray and (**b**) coating processes

calcium are found. In addition, small amounts of magnesium, sodium, and chlorine are present.

Figure 6 gives the EDX analysis of the prepared composites after abrasion process by medium grains and politex resin using spray and coating techniques. Indeed, after the abrading process, there was a decrease in the Fe peaks, which indicated that the abrading action of the surface is done by tearing off the iron grains. The increase in C, O, and Al peaks may be due to the presence of cavities, which allow waste from the piece to be polished to penetrate the amorphous part of the composites [30].

### 3.4 Thermal analysis

Thermogravimetric curves related to the reinforcement, the matrix (Politex), and iron medium grains are presented in Fig. 7. The TGA and the corresponding DTG curves of a pure non-woven show a single-step thermal degradation at 340 °C corresponding to the thermal hydrolysis of the cellulose [31]. Politex resin's DTG curve demonstrates the decomposition at different temperatures. Urethane bond rupture, which occurs at 135 °C, is responsible for the first mass loss. Between 100 and 200 °C, a fast weight loss of 60% was noted. From the DTG curve, a significant exothermic peak at 100 °C is seen. The second one at 350 °C is related to the ester group decomposition [32]. All urethane groups break down above 400 °C, and the final deterioration of the PU is caused by the breakdown of the urea group [33]. Based on Fig. 7 c, the thermogravimetric analysis of grains revealed a significant weight loss (about 35%) at 300 °C which is based on the total mass of iron [34]. This result proves the good resistance of iron grains to heat [35].

### 3.5 Surface roughness

The surface roughness results were summarized in Table 2. In fact, this parameter has a significant impact on the material removal process along with the types of polishing. The samples differ by the particle size of the grains, the type of process considered, and the choice of resin. As grain size increases, there is a greater fluctuation in the surface roughness value. If the grain size is sufficiently large, the increase in indentation depth may increase surface roughness [36, 37]. Shadab et al. demonstrated an improvement in surface roughness using large iron particles [10]. The values found herein show that there was not much improvement in surface roughness when changing the resin and the process type. The surfaces of the samples obtained by the spraying process are rougher compared to those obtained by the coating process. Indeed, the injection of the grains by a spray gun is manual, which makes it possible to create superimposed layers of grains resulting in non-uniform surfaces as shown by the SEM imagery illustrated in Fig. 3 a and EDX analysis given in Fig. 5 a. On the other hand, the coating process allows the

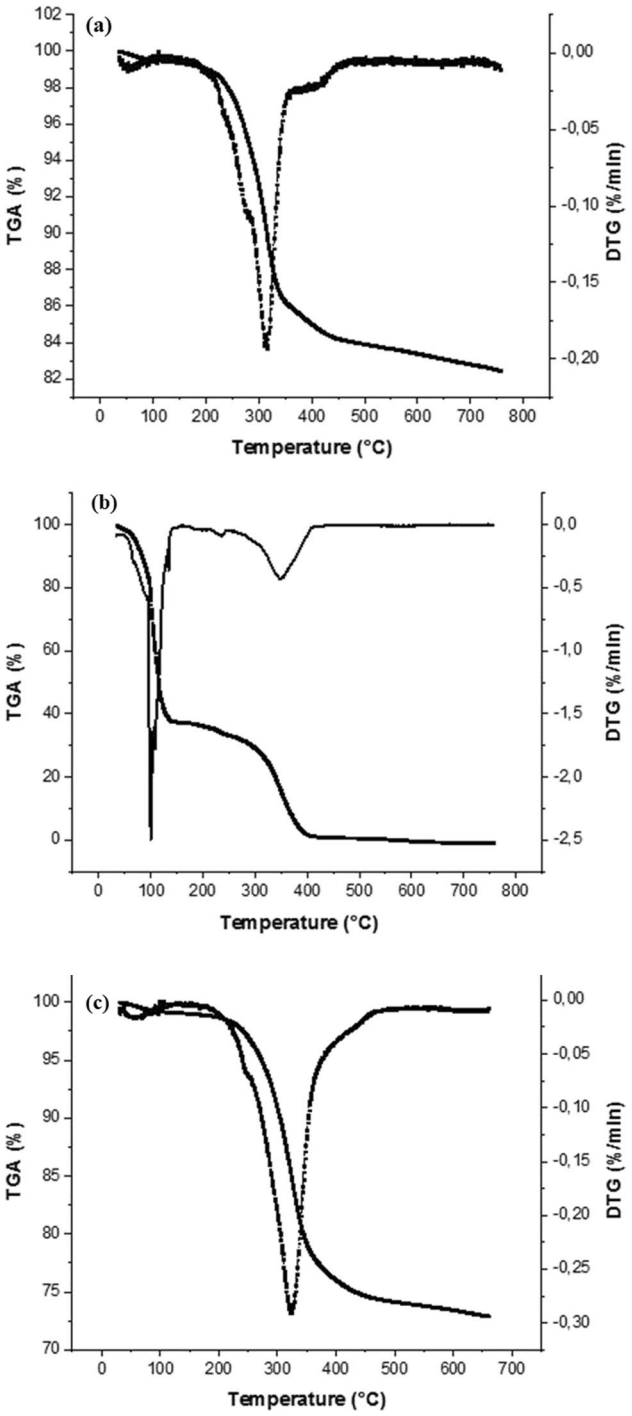


**Fig. 7** TGA/DTG curves of (**a**) non-woven, (**b**) Politex resin, and (**c**) iron medium grains

sedimentation of the particles over the entire surface in a more uniform way [38, 39].

### 3.6 Abrasive wear rate measurement

This analysis is performed on abrasives manufactured as shown in Table 1. According to Fig. 8, it is clearly observed that as the grits of the abrasives get larger, the abrasion process becomes more efficient and faster in scraping the fabric. For example, sample 7, which consists of large iron grains, and politex resin and obtained by spraying process, admits better results compared to sample 1 obtained by small iron grains in the same conditions [28]. In this context, Singh et al. [28] studied the influence of abrasive grain size on the wear of metallic materials. Depending on the use of abrasives, for example for a finishing or polishing process, the choice of grain size is necessary [40]. For the application of abrasives with large irons, it is found that the loss of abrasive mass is greater. Indeed, the grains are large so they are more apt to tear due to the size of the particle [41]. The measurements calculated for the spraying process are lower than those calculated for the coating process. This effect can be explained by the structural defects caused by the spraying process which is due to the arbitrary injection of the grains by the spray gun. We can infer that the coating process promotes adhesion between product components compared to the spraying proces. Politex resin has the best scraping and adhesion results between the components of the composite. This result is described by the flexibility and good adhesion of the polyurethane resin with the cellulosic nonwoven.

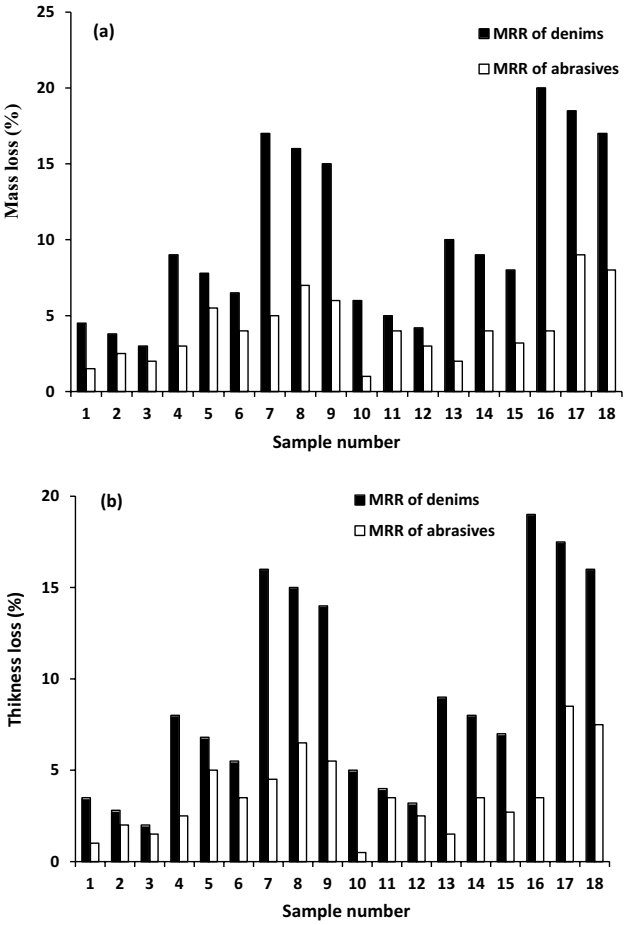


**Fig. 8** Effect of polishing with iron grain made abrasives: (**a**) mass loss and (**b**) thickness loss

**Table 2** Roughness values related to the studied samples

| Samples | Resin | Grains | Process | $R_Z$ (µm) | SD |
|---|---|---|---|---|---|
| 1 | Politex | Small size | Spraying | 450 | 0.52 |
| 2 | Resacryl M | Small size | Spraying | 430 | 0.63 |
| 3 | Polyester | Small size | Spraying | 420 | 0.94 |
| 4 | Politex | Medium size | Spraying | 890 | 0.88 |
| 5 | Resacryl M | Medium size | Spraying | 875 | 0.72 |
| 6 | Polyester | Medium size | Spraying | 870 | 0.43 |
| 7 | Politex | Large size | Spraying | 1320 | 0.82 |
| 8 | Resacryl M | Large size | Spraying | 1300 | 0.69 |
| 9 | Polyester | Large size | Spraying | 1290 | 0.47 |
| 10 | Politex | Small size | Enduction | 400 | 0.55 |
| 11 | Resacryl M | Small size | Enduction | 360 | 0.54 |
| 12 | Polyester | Small size | Enduction | 395 | 0.67 |
| 13 | Politex | Medium size | Enduction | 870 | 0.58 |
| 14 | Resacryl M | Medium size | Enduction | 850 | 0.66 |
| 15 | Polyester | Medium size | Enduction | 860 | 0.98 |
| 16 | Politex | Large size | Enduction | 1300 | 0.83 |
| 17 | Resacryl M | Large size | Enduction | 1245 | 0.72 |
| 18 | Polyester | Large size | Enduction | 1265 | 0.58 |

## 4 Conclusion

In this study, low-cost abrasives with a good performance were prepared using spraying and coating techniques. The properties of the matrices, process considered, size of the grains, and their distribution were the principal parameters affecting the abrasive process. FT-IR spectra confirmed the adhesion between the non-woven, resin, and abrasive grains. SEM analyses proved the effect of abrasion on the surface of abrasives. After the abrading process, the EDX analysis suggested that the abrading action of the surface might be done by tearing off the iron grains. The evaluation of the mechanical analysis (abrasion test) indicated that the abrasives produced by the coating process have better abrasion resistance compared to those obtained by the spraying process. The roughness and surface morphologies of abrasives are mainly affected by the type and size

of the abrasives. The abrasives can be categorized based on the intended polishing. In the sanding process, large grits can be used. Small-scale grains are suited for finishing operations.

**Author contribution** Arwa Elaissi: Conceptualization, Methodology, Software, Data curation, Writing—original draft. Mahjoub Jabli: Methodology, Software, Data curation, Writing—original draft. Adel Ghith: Software, Data curation, Visualization, Investigation.

**Data availability** Data sharing does not apply to this paper.

## Declarations

**Ethical approval** Consent to participate not applicable.

**Conflict of interest** The authors declare no competing interests.

## References


1. Brookes KJ (1992) World directory and handbook of hardmetals and hard materials. International Carbide Data, World Directory and Handbook of Hardmetals and Hard Materials, 5th edn. International Carbide Data, p 463
2. Antonov M, Veinthal R, Yung DL, Katušin D, Hussainova I (2015) Mapping of impact-abrasive wear performance of WC–Co cemented carbides. Wear 332:971–978
3. Hussainova I, Antonov M, Voltsihhin N, Kübarsepp J (2014) Wear behavior of Co-free hardmetals doped by zirconia and produced by conventional PM and SPS routines. Wear 312:83–90
4. Rabinowicz E, Dunn L, Russell P (1961) A study of abrasive wear under three-body conditions. Wear 4:345–355
5. Krikar M, Gharrib Noori HHI (2018) Mechanical properties of concrete using iron waste as a partial replacement of sand. In: 4th International Engineering Conference on Developments in Civil & Computer Engineering Applications, pp 204–215
6. Ugama T, Ejeh S, Amartey D (2014) Effect of iron ore tailing on the properties of concrete. Civ Environ Res 6:7
7. Ghannam S, Najm H, Vasconez R (2016) Experimental study of concrete made with granite and iron powders as partial replacement of sand. Sustain Mater Technol 9:1–9
8. Leo Kumar SP, Jerald J, Kumanan S, Prabakaran R (2014) A review on current research aspects in tool-based micromachining processes. Mater Manuf Process. 29:1291–1337
9. Rakhimyanov KM, Semenova I (2016) Surface state control by ultrasonic plastic deformation at the final machining stage. Mater Manuf Process 31:764–769
10. Ahmad S, Gangwar S, Yadav PC, Singh DK (2017) Optimization of process parameters affecting surface roughness in magnetic abrasive finishing process. Mater Manuf Process 32:1723–1729
11. Xiangdong F, Dean SC, Wang ZL, Paras MS, Santora B, Sutorik AC, Sayle TXT, Yang Y, Ding Y, Wang X, Her Y-S (2006) Her Converting ceria polyhedral nanoparticles into single-crystal nanospheres. Sciences 312:1504–1508
12. Jayswal S, Jain V, Dixit P (2005) Modeling and simulation of magnetic abrasive finishing process. Int J Adv Manuf Technol 26:477–490
13. Suzuki H, Kodera S, Hara S, Matsunaga H, Kurobe T (1989) Magnetic field-assisted polishing—application to a curved surface. Precis Eng 11:197–202
14. Baley C (2002) Analysis of the flax fibres tensile behaviour and analysis of the tensile stiffness increase. Compos Part A: Appl Sci Manuf 33:939–948
15. Summerscales J, Dissanayake NP, Virk AS, Hall W (2010) A review of bast fibres and their composites. Part 1–Fibres as reinforcements. Compos Part A: Appl Sci Manuf 41:1329–1335
16. Elaissi A, Alibi H, Ghith A, Legrand X (2022) The impact of chemical treatment of cellulosic fibers on surface properties and matrix/reinforcement interfacial adhesion. J Nat Fibers 19:11560–11573
17. Elaissi A, Alibi H, Jabli M, Ghith A (2022) Development of abrasives from non-woven based on used textiles. J Nat Fibers 19:2189–2203
18. Roper HJ (2004) Surface preparation for optimum thermal spray adhesion and long life. NACE CORROSION
19. Narayanaswamy B, Hodgson P, Beladi H (2016) Effect of particle characteristics on the two-body abrasive wear behaviour of a pearlitic steel. Wear 354:41–52
20. Škoc MS, Pezelj E (2012) Abrasion resistance of high performance fabrics. Abrasion resistance of materials. InTech, Rijeka, pp 35–52
21. Rouchon V, Badet H, Belhadj O, Bonnerot O, Lavédrine B, Michard JG, Miska S (2012) Raman and FT-IR spectroscopy applied to the conservation report of paleontological collections: identification of Raman and FTIR signatures of several iron sulfate species such as ferrinatrite and sideronatrite. J Raman Spectrosc 43:1265–1274
22. Namduri H, Nasrazadani S (2008) Quantitative analysis of iron oxides using Fourier transform infrared spectrophotometry. Corros Sci 50:2493–2497
23. Schwertmann U, Cornell RM (2008) Iron oxides in the laboratory: preparation and characterization. John Wiley & Sons
24. Trovati G, Sanches EA, Neto SC, Mascarenhas YP, Chierice GO (2010) Characterization of polyurethane resins by FTIR, TGA, and XRD. Sci Res 115:263–268
25. Pathania D, Sharma R, Kalia S (2012) Graft copolymerization of acrylic acid onto gelatinized patato starch for removal of metal ions and organic dyes from aqueous system. Adv Mater Lett 3:259–264
26. Misawa T, Kyuno T, Suetaka W, Shimodaira S (1971) The mechanism of atmospheric rusting and the effect of Cu and P on the rust formation of low alloy steels. Corros Sci 11:35–48
27. Fan Q (2005) Chemical testing of textiles, 1st edn. Elsevier, Woodhead Publishing Series in Textiles
28. Singh RK, Telang A, Das S (2022) The influence of abrasive size and applied load on abrasive wear of Al-Si–SiCp composite. Arab J Sci Eng 47:8617–8628
29. Sabarinathan P, Annamalai V, Rajkumar K (2020) Sustainable application of grinding wheel waste as abrasive for abrasive water jet machining process. J Clean Prod 261:121225
30. Wahab MA, Boubakri H, Jellali S, Jedid, (2012) Characterization of ammonium retention processes onto Cactus leaves fibers using FTIR, EDX and SEM analysis. J Hazard Mater 241–242:101–109
31. Goriparthi BK, Suman K, Rao NM (2012) Effect of fiber surface treatments on mechanical and abrasive wear performance of polylactide/jute composites. Compos Part A: Appl Sci Manuf 43:1800–1808
32. Trovati G, Sanches EA, Neto SC, Mascarenhas YP, Chierice GO (2010) Characterization of polyurethane resins by FTIR, TGA, and XRD. 115:263-268
33. Solarski S, Benali S, Rochery M, Devaux E, Alexandre M, Monteverde F, Dubois P (2005) Synthesis of a polyurethane/clay nanocomposite used as coating: Interactions between the counterions of clay and the isocyanate and incidence on the nanocomposite structure. J Appl Polym Sci 95:238–244

34. Scaccia S, Carewska M, Prosini PP (2004) Thermoanalytical study of iron (III) phosphate obtained by homogeneous precipitation from different media. Thermochim Acta 413:81–86
35. Hara K, Matsushita T, Nagata KJI (2013) In-situ X-ray transmission observation of carbothermic reduction of magnetite powder and macroscopic agglomeration of reduced iron. ISIJ Int 53:1010–1019
36. Jain RK, Jain VK, Dixit P (1999) Modeling of material removal and surface roughness in abrasive flow machining process. Int J Mach Tools Manuf 39:1903–1923
37. Jain R, Jain V, Kalra P (1999) Modelling of abrasive flow machining process: a neural network approach. Wear 231:242–248
38. Narcisa V, Iorgoaiea GM, Christine C, Giraud S, Prepilita RI, Coman D, Petrescu VD, Dumitrascu DD, Ouerfelli N, Suchea MP (2018) Correlation between surface engineering and deformation response of some natural polymer fibrous systems. J Eng Fibers Fabr 13:155892501801300200
39. Narayan P, Hancock BJMS (2005) The influence of particle size on the surface roughness of pharmaceutical excipient compacts. Mater Sci Eng A 407:226–233
40. Kök M (2006) Abrasive wear of $Al2O_3$ particle reinforced 2024 aluminium alloy composites fabricated by vortex method. Compos Part A: Appl Sci Manuf 37:457–464
41. Tong J, Ma Y, Arnell RD, Ren L (2006) Free abrasive wear behavior of UHMWPE composites filled with wollastonite fibers. Compos Part A: Appl Sci Manuf 37:38–45